Do not type or paste anything outside this line. Type up to, but not beyond, the blue margin lines at left and right

Optical and electrical properties of reactively sputtered TiN, ZrN, and HfN thin films

Samad M. Edlou and John C. Simons
Barr Associates, inc., 2 Lyberty Way, Westford, MA 01886

and

Ghanim A. Al-Jumaily and Nasrat A. Raouf
Jet Propulsion Laboratory, 4800 Oak Grove Drive, Pasadena, CA 91109

ABSTRACT

Thin films of titanium, zirconium and hafnium nitride are prepared by DC magnetron reactive sputtering at room temperature on fused silica, optical glass and silicon substrates. Deposition parameters are investigated in order to obtain stoichiometric films, The optical and electrical properties of the films as a function of nitrogen partial pressure are determined. The results show that an inverse correlation exists between the optical reflectance and the electrical resistivity of the films. The optical constants of the films are determined by Variable Angle Spectroscopic Ellipsometry (VASE) measurements from 240--1700 nm at 10 nm steps. Deposited film composition is obtained by the Rutherford Ion Back Scattering (RBS) method. The rms roughness of the films is measured by using an optical scatterometer. Ellipsometer data for all three films show that their refractive index (n) in the visible spectrum is decreased by increasing the film thickness while the extinction coefficient (k) is unchanged. Thin films of TiN have the lowest room temperature resistivity ($\cong 75\ \mu\Omega$ - cm) relative to ZrN and HfN thin films.

Keywords: Reactive sputtering, optical coatings, optical properties, electrical properties, thin films, transition metal nitrides.

1. INTRODUCTION

Titanium nitride (TiN), zirconium nitride (ZrN) and hafnium nitride (HfN) have optical, electrical and mechanical properties[1-6] that are advantageous for applications to optics, electronics and tribology. Generally, nitride films have been deposited by chemical vapor deposition (CVD) or physical vapor deposition (PVD). However, CVD involves high temperature processing and PVD produces porous films with poor adhesion. Two other deposition methods have also been employed for making nitride coatings: magnetron reactive sputtering[7-10] and electron cyclotron resonance (ECR) deposition.[11-12] In recent years magnetron sputtering in recent years has become the leading coating process, compared to CVD and PVD because of these advantages:

- Magnetron sputtering can be done from large-area targets with different geometry, which simplifies the problem of coating of large area substrates with uniform film thickness;
- The composition of sputter-deposited films can be tightly controlled;
- The device damage from X-rays generated during electron beam evaporation is eliminated;
- Coatings can be accomplished at relatively higher deposition rates; and
- Fully dense films are produced at room temperature,

Do not type or paste anything outside this line. Type up to, but not beyond, the blue margin lines at left and right

The aim of this work was to produce nitride films with desirable optical, electrical and mechanical properties that can survive harsh environments. The most important objective was to develop a reactive magnetron sputter deposition process at room temperature for TiN, ZrN, and HfN films that yields a coating with the following properties:

- Reflectance from the UV to far-n{ optical range with values near theoretical maximum;
- Good adherence to substrates, particularly fused silica, optical glass and silicon;
- Low scatter films; and
- Hard coatings.

2. SAMPLE PREPARATION

The DC magnetron sputtering system we set up meets our requirements for stability, good uniformity, ability to produce multi layer films, and high production rates. The system is a 76 x 76 x 61-cm box coater with a mechanical roughing pump and a 30 cm-diameter high-vacuum cryopump with a water vapor pumping speed of 10,000 liters per second, This high pumping speed prevents reactive gases from poisoning the target material and helps achieve stability. The system's lowest attainable base pressure is 3 x 10-8 torr. Two 15 cm- and one 8 cm-diameter magnetron cathodes are mounted at the bottom of the deposition chamber, meeting the demand for producing multilayer films with good uniformity. This arrangement makes it possible to deposit nitrides, oxides, and compounds of three materials without venting the chamber. Up to three gases can be flowed into the chamber at any given time. The reactive and working gases used in the process are ultra-high-purity grade 5. Flow rates of the gases into the chamber are controlled separately by precision mass flow valves permitting Ar:N2, Ar:02 and N2:02 ratios to be varied at will. The system is equipped with both an optical and a quartz crystal monitor, enabling control of the deposition rate by either method.

All three starling materials are metal targets with 99.95 ?/o purity. The substrates arc not intentionally heated or biased during deposition, 10 the reactive sputtering process an argon flow of 25 seem (cubic centimeter pcr minute at S'J'J') and a nitrogen gas flow of 3, 5, 10, 15, 20, 25, or 30 seem arc used, resulting in a deposition pressure in the range of 2.8- 5 x 10-" torr. Coatings are deposited onto optical glass, fused silica, and silicon substrates. The deposition rate for all three coatings is 3-5Å/sec with a source-to-substrate distance of 25 cm. All depositions started at a base pressure of 6 x 10^{-7} torr.

3. DETERMINATION OF OPTICAL CONSTANTS USING ELLIPSOMETRY

3.1 Samples

For each material, four samples are prepared on fused silica substrates. Two of the films are intended to be optically thick (opaque), while the other two were much thinner at 30 40 nm. For each type (thick and thin), one of the substrates was roughened on the back side, while the other was left smooth.

3.1.2 Measurements

Variable angle spectroscopic ellipsometry (VASE) measurements Were made on all samples from 240 nm to 1700 nm at 10 nm *steps* at external angles of incidence (ϕ_0) of 70, 75, and 80° using a commercial rotating analyzer-type ellipsometer. Some small artificial oscillations occur in VASE data at long wavelengths due to imperfections in the polarizers. As a result, small oscillations also occur in the derived *n* and *k* data at long wavelengths. No attempt was made to smooth the data.

This is the last line of the page. Do not type or paste below this line.

Do not type anything on this line.

100% SPIE MANUSCRIPT SHEET SPIE CODE NO. IS STAMPED ON BACK

Do not type or paste anything outside this line. Type up to, but not beyond, the blue margin lines at left and right.

3.2 Analysis

3.2.1 Thick samples

Transmittance data confirmed that the thicker films were opaque ($T \approx 0$ over the ent ire 240--1700 nm spectral range). '1'bus, these films could be treated as substrates since the light did not penetrate to the fused silica interface. For a simple substrate, the ellipsometric data can be converted directly into a pseudodielectric function ε using

$$\varepsilon = \sin^2\phi_0\left[1 + \left(\frac{1-\rho}{1+\rho}\right)^2\tan^2\phi_0\right], \qquad (1)$$

where $\rho(\lambda, \phi_0)$ is the measured complex ellipsometric parameter, usually given in terms of two angles, Ψ and Δ.

$$\rho = \tan\Psi e^{i\Delta}. \qquad (2)$$

To the extent that the surface is perfectly smooth and has no overlays, as assumed here, the pseudodielectric function and the true dielectric function arc ident ital. Corresponding pseudo-values for n and k arc found from:

$$\varepsilon = \varepsilon_1 + i\varepsilon_2 = N^2 = (n + ik)^2. \qquad (3)$$

Pseudo-values from different angles ϕ_0 arc identical (except from random noise), so the average over all angles was taken.

3.2.2 Thin samples

In this case the exact thickness (t) and n and k at each wavelength (λ) arc unknown. VASE data were analyzed using a one-film model in which the fused silica substrate's optical constants arc known, and initial guesses for t, $n(\lambda)$, and $k(\lambda)$ of the film arc given. The ellipsometric parameter ρ is calculated from:

$$\rho = \frac{R_p}{R_s}, \qquad (4)$$

where R_p (R_s) is the complex reflection coefficient for light polarized parallel (perpendicular) to the plane of incidence, These were calculated from the one film model using standard formulas. The values of t, $n(\lambda)$, and $k(\lambda)$ were varied to get a best-fit to the data, using a χ^2 minimization algorithm.

Correlation between t and the film's optical constants is a typical problem in the fitting. That is, there is no unique set of t, n anti k that produces the same or nearly the same best fit to VASE data. Simultaneously fitting both VASE anti T data removes the correlation. (This was the reason for preparing the thin films on transparent substrates.) The approach worked well. We obtained good tit for both VASE and T spectra with unique best-fit, t, anti n and k values, As an independent check, n and k data were used to fit the VASE data from the thin layer samples with roughened' substrate backsides using only t as a fitting parameter. We obtained very good fits, indicating that n and k fitted values were reasonably accurate.

3.2.3 Lorentz oscillator model

in addition to fitting n and k individually at each wavelength, a simple Lorentz oscillator model was used to fit n and k with only a few wavelength-independent parameters. In this model, ε of the film (either thick or thin) was modeled as:

$$\varepsilon(E) = \varepsilon_\infty + \sum_{i=1}^{n}\frac{A_i}{E^2 - E_i^2 + j\Gamma_i E}, \qquad (5)$$

This is the last line of the page. Do not type or paste below this line.

Do not type anything on this line

PRO 30/61 Author name(s) LEDLOU

where $E = h\nu$ is the photon energy, and E, and Γ_i are the center energy and broadening parameter, respectively, of the i-th oscillator. All energies are in eV, and the amplitude A_i has a unit (eV)*. Only two oscillators were used for all three materials. The first oscillator was located at E_1 = O, corresponding to the free electron response (Drude model). The other was located at higher energy (≈6 eV), beyond our spectral range, to account for interband transitions in the UV.

S. RESULTS AND DISCUSSION

5.1 Optical constants of transparent (thin) and opaque (thick) film

Fitted oscillator parameters are given in Table 1 for thick (TK) and thin (TN) films of each material. All oscillator parameters, except E_1 which was fixed to O eV, were fixed to the values found from the wavelength-by-wavelength fitting combining VASE and transmittance data,

Table 1. Two-oscillator fitted parameters.

	HfN		ZrN		TiN	
	TK	TN	TK	TN	TK	TN
ε_∞	2.74	3.11	2,31	2.42	**0.79**	**1.89**
A_1 (eV)*	**65**	**70**	6 2	65	52	57
1 't (eV)	0.9	1.20	0.73	0.95	0,71	0.83
E_1 (eV)	0	**0**	" o	o	0	0
A_2 *	99	101	·124	153	202	160
"2	2.8	3.8	·2.7	4.2	4.3	4
E_2	6.1	6.2	·6.1	6.6,	6.3	5.8
χ^2	3 . 8	27	,2,7	22,	9.8	15
t (nm)	---	39.5	--	40.7	---	34.1

Note the values of χ^2 which indicate how good the fits were. The oscillator model works well for ZrN and HfN thick films (low χ^2), but not nearly as good for thin films. It also works less well for the TiN thick film. Figures 1 and 2 show real (n) and imaginary (k) parts of the complex index of refraction for thick (TK) TiN, ZrN, and HfN films determined by VASE over the spectral wavelength of 240 1700 nm respectively. Notice in Figure 1 that the real parl of the refractive index, n, is close to or below 1 in the major part of the visible spectrum (440- 670 rim).

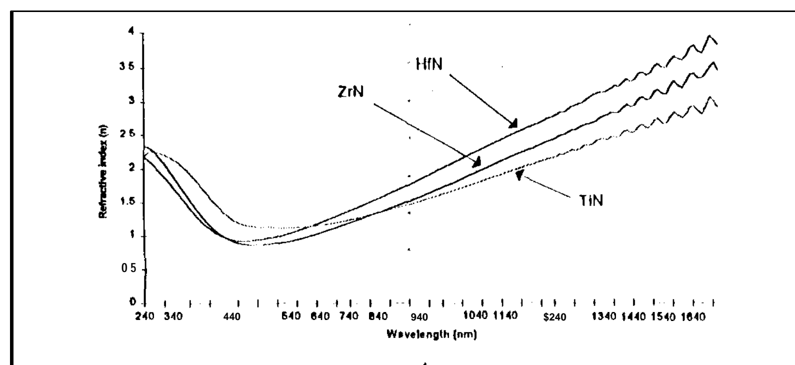

Figure 1. Real part of the refractive index of TK TiN, ZrN and HfN.

100% SPIE MANUSCRIPT SHEET   SPIE CODE NO. IS STAMPED ON BACK

Do not type or paste anything outside this line. Type up to, but not beyond, the blue margin lines at left and right

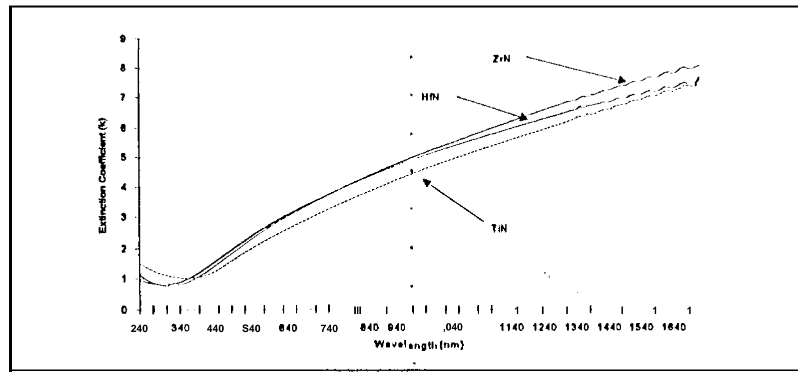

'igure 2. *Imaginary part of refractive index of TK • TiN, ZrN and HfN.*

Figures 3, 4 and S compare n and k values for thick and thin films of TiN, ZrN and HfN respectively. Results show that optical constants for the films, prepared at the same deposition conditions, not only depend on the wavelength of light, but also on the thickness, t, of the films. TiN shows less difference between thick and thin film optical constants and the difference is distributed differently than for the other two materials. The results imply that n and k arc functions of the film's thickness, at' least over some range of thickness with ZrN and HfN, and to a lesser extent with TiN. Most of the dependence on thickness is in the longer wavelength regions where free electron absorption dominates. If in particular applications all films arc to be very thick (hundreds of m), then the variations of n and k in the films are minimal.

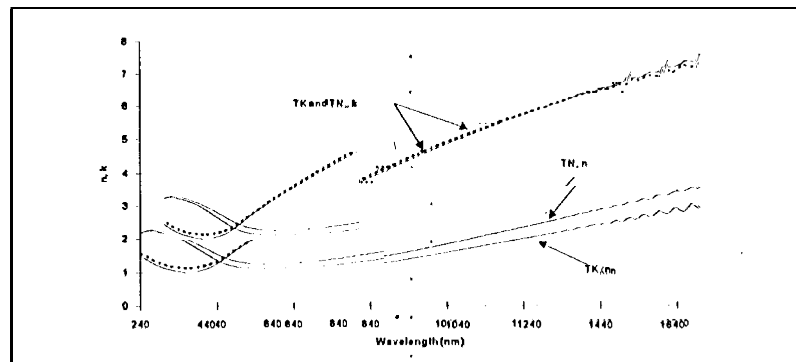

'igure 3. *Optical constants of TK • and TN • TiN measured with VASE.*

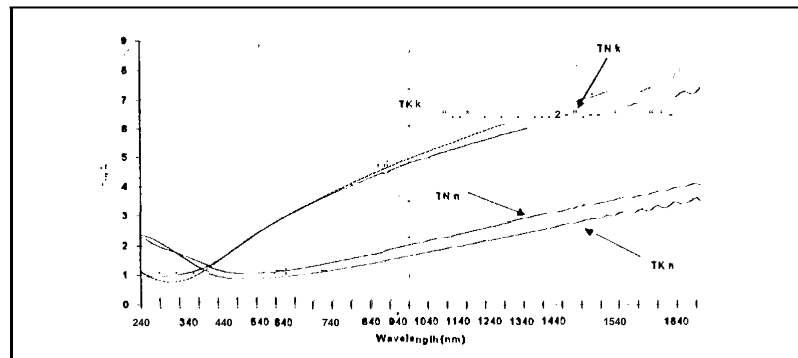

'igure 4. *Optical constants of TK • and TN • ZrN measured with VASE*

This is the last line of the page. Do not type or paste below this line.

Do not type anything on this line

Do not type or paste anything outside this line. Type up to, but not beyond, the blue margin lines at left and right

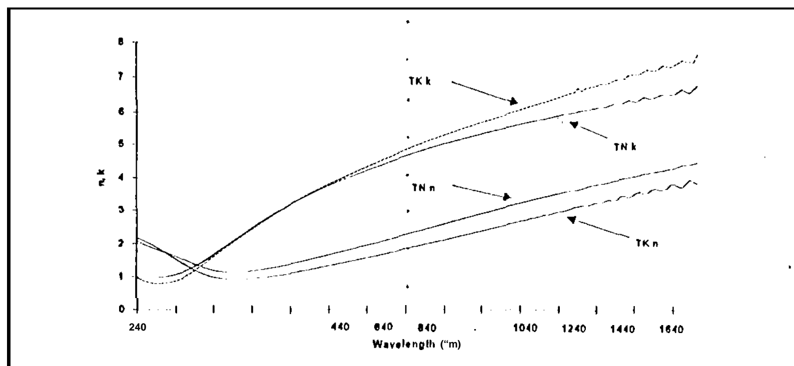

Figure 5. Optical constants of TK • and TN • HfN measured with VASE,

The spectral reflectance and transmittance of the three nitride films are calculated using a commercial film design software package where the input data are the measured *n, k,* and film thickness *t*. The films arc assumed to be coated on a non-absorbing fused silica substrate with $n_s = 1.46$. Figures 6-8 present the calculated spectral reflectance and transmittance as a function of wavelength for these films. The results imply that the spectral behavior of TiN, ZrN and HfN films are similar to the noble metals Au, Ag and Pt. Reflectance curves increase slowly with increasing wavelength, approaching their maximum of ~93% in the infrared. The transmittance curves increase slowly with decreasing wavelength towards a maximum in the mid-lower side of the visible spectrum and there is a corresponding reflectance minimum at these wavelengths. If we compare the reflectance and transmittance of these three nitrides to that of noble metals, TiN is most similar to Au, and HfN and ZrN are similar to Ag.

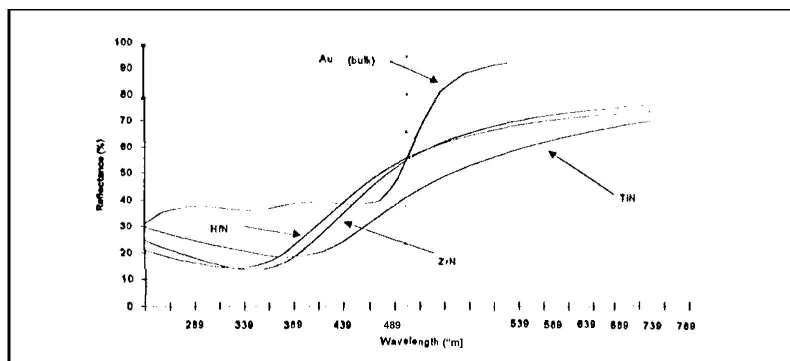

Figure 6. Spectral reflectance vs. wavelength for thin films of TiN, ZrN, H' and bulk Au.

This is the last line of the page. Do not type or paste below this line

Do not type anything on this line.

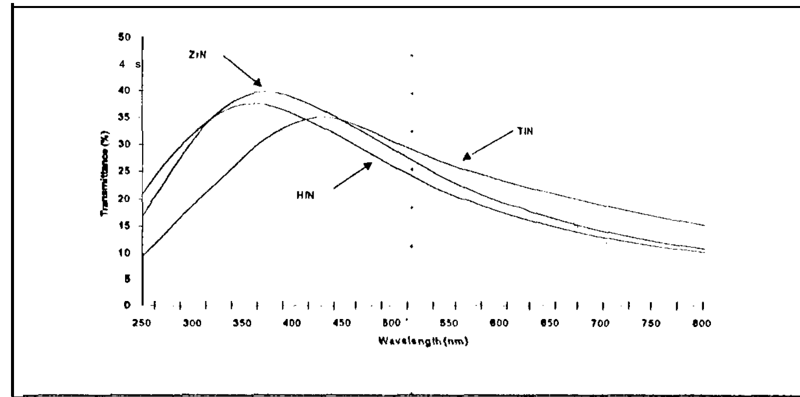

Figure 7. Spectral transmittance of thin films of TiN, ZrN and HfN.

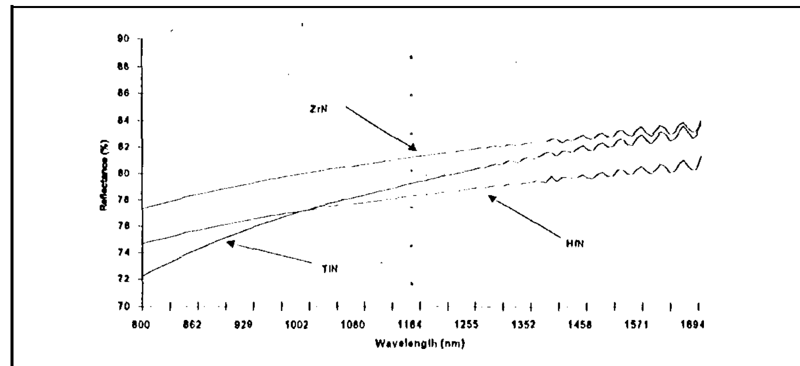

Figure 8. Calculated reflectance of TiN, ZrN and HfN thin films at normal incidence.

5.2 Composition analysis

Film composition was obtained by Rutherford backscattering analysis. The amounts of metal, nitrogen and oxygen were determined quantitatively from the areas beneath the spectra peaks and from the Rutherford cross-section of each element. The composition of the films with and without ECR is listed in Table 2. Oxygen is the main impurity in all films. It may be assumed that this is due to the residual pressure of oxygen in the chamber. The ratio of nitrogen to oxygen increases with the atomic weight of the starting material, HfN, with the heaviest atomic weight, has the highest nitrogen-to-oxygen atomic ratio.

5.3 Optical Scatter Characterization

Two depositions were made for each material -- one with and one without ECR --- onto super-polished fused silica substrates. We examined scattering from each coating using an angle-resolved optical scatterometer at the University of New Mexico. As shown in Table 3, TiN and HfN coatings have rms roughness similar to super-polished substrates; ZrN has much higher rms. One reason for this could be due to its crystalinity.

100% SPIE MANUSCRIPT SHEET — SPIE CODE NO. IS STAMPED ON BACK

Do not type or paste anything outside this line. Type up to, but not beyond, the blue margin lines at left and right

Table 2. RBS results of 2 Mev He^+ ions on TiN, ZrN, and HfN films on graphite substrate.

Film	Thickness (Å)	Ti	N	O	Zr	Hf	Ar
		Film Composition (at%)					
TiN	48	48	48	4	0	0	0
TiN	962	48	48	4	0	0	0
TiN w/ECR	916	48	48	4	0	0	0
ZrN	102	0	42	15	43	0	0
ZrN	140	0	49	8	43	0	0
ZrN	386	0	52	4	44	0	0
ZrN w/ECR	53	0	51	6	43	0	0
ZrN w/ECR	235	0	50	5	45	0	0
ZrN w/ECR	430	0	49	4	47	0	0
HfN	82	0	53	4,7	4.4	36	1.9
HfN	344	0	51	4.6	4.5	38,4	1,5
HfN	1335	0	52	4	4	40	0
HfN w/ECR	128	0	48	5	4.8	40.5	0.7
HfN w/ECR	450	0	47	2.5	4.5	44	1

Table 3. Rms roughness values obtained using an optical scatterometer.

	rms Roughness (Å) Trial Number 1	2	3	Average	Standard Deviation
TiN	26.4	14.0,	12	17.5	7.8
TiN w/ECR	10.6	7.4	—	9.0	2.3
ZrN	27.5	76.3	27.9	43.9	28.1
ZrN w/ECR	23.0	35,1	46.1	34,7	11.6
HfN	14.7	9.1	-	11.9	4
HfN w/ECR	25.3	25.0	-	25.2	0.2

5.4 Electrical resistivity

Measured sheet resistance (R_s) of the films as a function of nitrogen gas flow rate during the deposition are listed in Table 4. Film resistivity calculated from R_s and film thickness, t, as a function of N_2 flow rate are plotted in Figures 9-11.

Table 4. Measured sheet resistance R_s of the nitride films.

N_2 Flow (sccm)	R_s (Ω) – TiN	R_s (Ω) – ZrN	R (Ω) – HfN
3	11.7	15	15
5	5	15	9.9
10	4.4	20	28
15	5.3	30	235
20	6	99	1100
25	7.7	120	14400
30	9	510	too high

This is the last line of the page. Do not type or paste below this line.

Do not type anything on this line.

EDLOU

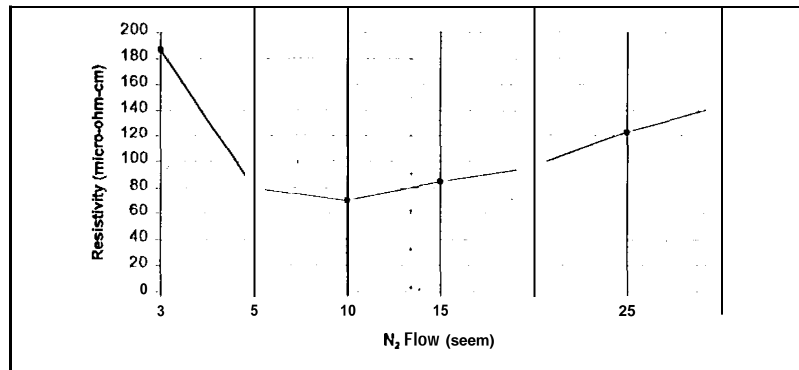

Figure 9. Room temperature resistivity of TiN as a function of nitrogen flow rate.

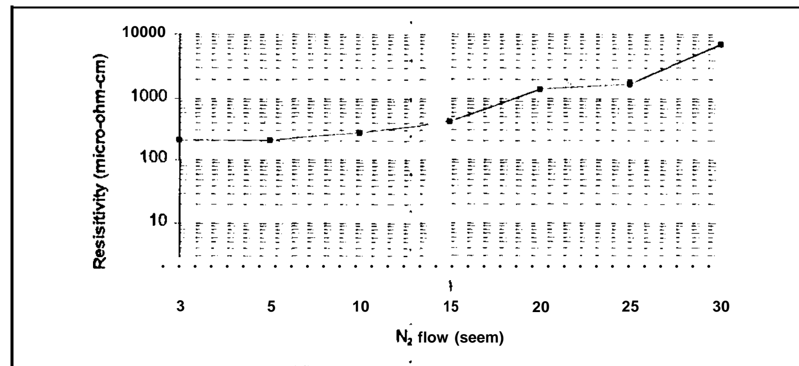

Figure 10. Room temperature resistivity of ZrN as a function of nitrogen flow rate.

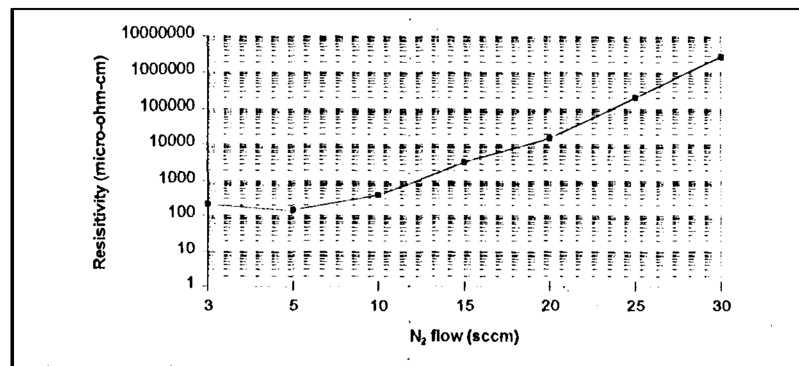

Figure 11. Room temperature resistivity of HfN as a function of nitrogen flow rate.

It is important to notice that there exists a critical nitrogen flow where the resistivity changes abruptly for ZrN and HfN, but has relatively much less effect in the case of TiN. in our investigation we found that there is a link between the color, resistivity and optical reflectance of the three films. For TiN, a nitrogen-to-titanium ratio of unity results in maximum reflectance with a gold color and minimum room temperature resistivity of 75 $\mu\Omega$-cm. For ZrN the atomic ratio of nitrogen to Zr is about 1,12 and for HfN the ratio is 1.30, resulting in *200* and 140 $\mu\Omega$-cm room temperature resistivity,

Do not type or paste anything outside this line. Type up to, but not beyond, the blue margin lines at left and right

respectively. By increasing or decreasing the N_2 flow the color changes to gray, optical reflectance drops, and resistivity increases in all three materials.

6. Durability

Deposited coatings of TiN, ZrN and HfN were subjected "to severe abrasion by rubbing the coated surfaces with a standard eraser conform ing to MI L-E- 12397 mounted in an eraser abrasion tester. ('l'his is a US Army specificat ion for hard coatings.) For the accelerated aging test the samples were put into an environmental controlled test chamber and exposed to a temperature of 65°C and 95–) 00% relative humidity for 120 hours. To test the thermal stability of the coatings, the TiN samples were baked in an oven for three hours at 300°C in air at atmospheric pressure. The coatings did not exhibit any evidence of scratches, flaking, peeling or blistering. However, the baked coating of TiN showed an approximate 3% reflectance drop in the 1.5 μm to 3.0 μm optical range. There was no reflectance drop in either the 0.2-1.5 μm or 3.0-32.0 μm optical ranges.

7. CONCLUSIONS

Reactive DC magnetron sputtering was used to prepare thin films of TiN, ZrN and HfN at room temperature. The films exhibit optical properties similar to noble metals. The ellipsometry data implies that the n and *k* of the films are a function of the film's thickness - - at least over some range of thickness for ZrN and HfN, and to a lesser extent with TiN, The composition of TiN, ZrN and HfN and their corresponding optical and electrical properties can be varied by controlling nitrogen partial pressure during deposition. The room temperature resistivity values obtained in this investigation for TiN, ZrN and HfN thin films are 75 μΩ-cm, 200 Ωμ-cm, and 140 μΩ-cm respectively. The process has the potential to produce TiN, ZrN and HfN with rms roughness comparable to that of super-polished substrates, i.e., 1- 5Å rms roughness. Film adhesion to fused silica, optical glass and silicon substrates is excellent. TiN films exhibit optical properties most similar to Au, while ZrN and HfN films are similar to Ag. Comparing the two groups, noble metals and the transition metal nitrides, we conclude that the transition metal nitrides exhibit superior mechanical and chemical properties, but not as good optical nor electrical properities.

8. ACKNOWLEDGMENTS

The work reported here was supported in part by NASA under SBIR Phase 11 Contract NAS7-1150, with technical support provided by the Jet Propulsion Laboratory. The authors wish to express their thanks to Paul Snyder of the University of Nebraska for conducting ellipsometry analysis, Wendy Kosik of tbc US Army Materials Laboratory at Watertown, Massachusetts for RBS measurements, J. R. McNeil and Scott Wilson of Sandia Systems, inc. for the scatterometer measurements, and Christine E. Bronson of Barr Associates, inc. for discussions and help in typing this manuscript.

This is the last line of the page. Do not type or paste below this line.

Do not type anything on this line

100% SPIE MANUSCRIPT SHEET SPIE CODE NO. IS STAMPED ON BACK

Do not type or paste anything outside this line. Type up to, but not beyond, the blue margin lines at left and right

9. REFERENCES

1, M. Veszelei, K. Anderson, C, G. Ribbing, K. Järrendahl and H. Arwin, "Optical constants and Drude model analysis of sputtered zirconium nitride films," Applied Optics, **10**, pp. 1993-2991 (1994).

2, Y. Claesson, M. Georgson, A. Roos and C. G. Ribbing, " Optical characterization of titanium nitride based on solar control coatings," Solar Energy Materials, 20, pp. 455-465 (1990).

3. N. Savvides and B. Windows, "Electrical transport, optical properties and structure of TiN films synthesized by low-energy ion-assisted deposition," J. Appl. Phys., 64, pp. 225-234 (1988).

4. D. S. Yee, J. J. Cuomo, M. A. Frisch and D. P. E. Smith, "Reactive radio frequency sputter deposition of higher nitrides of titanium, zirconium and hafnium," J. Vat. Sci. Technol. A4, **3**, pp. 381-387 (1988).

5. W. D. Sproul, "Reactively sputtered nitrides and carbides of titanium, zirconium and hafnium," J. Vat, Sci. Technol. 4,6, pp. 2874-2878.

6. A. Schlege, P. Wachter, J. J. Nick and H. Lingg, "Optical properties of TiN and ZrN," J. Phys. C: Solid State Phys., 10, pp. 4889-4895 (1977).

7. S. Berg, H. 0. Blom, M. Moradi and C. Nender, "1'recess modeling of reactive sputtering," J. Vat. Sci. Technol. A7, **3**, pp. 1225-1229.

8. B. Chapman, Glow Discharge Processes, 1st Edition, Chap. 6, pp. 177-283 (J. Wiley, New York, 1980).

9. R. Parson, "Sputter deposition processes," II-4, pp. 177-204 in Thin Film Processes, edited by J. J. Vossen and W. Kern (Noyes Publications, New Jersey, 1991).

10. K. Wasa and S. Hayakawa, Handbook of Sputter Deposition Technology: Technology, Principles and Applications (Noyes Publications, New Jersey, 1992).

11. P. Bai, J. Liu, N. Parikh and M. Swanson, "Characterization of electron cyclotron resonance microwave plasma under critical configuration of magnetic field," J. Vat. Sci. Technol. A, 12, 1, pp. 114-119.

12. S, Mat sue, "Microwave electron cyclotron resonance plasma chemical vapor deposit ion," Chap. 5, pp. 147--168, in Handbook of Thin Film Deposition Processes and Techniques, edited by K. K. Schuegraf (Noyes Publications, New Jersey, 1988).

13. Z. Knittl, Optics of Thin Films (An Optical Multilayer Theory), Chap. 3, pp. 69-148 (John Wiley, New York, 1976).

14. H. A. Macleod, Thin Film Optical Filters, 2nd Edition, Chap. 5, pp. 158-186 (McGraw-Hill, New York, 1986).

15. A. Thelen, Design of Optical Interference Coatings, Chap. 5, pp. 109-122 (McGraw-Hill, New York, 1989).

16. O. S. Heaven, Optical Properties of Thin Solid Films, Chap. 4, pp. 46-95 (Dover, New York, 1991).

17. G. Hass, "Mirror coat ings," Chap. 8, pp. 309-330, in Applied Optics and Optical Engineering, Vol. III, edited by R. Kingslake (1965).

This is the last line of the page. Do not type or paste below this line.

Do not type anything on this line.

FED LOU